Fluid Mechanics: Numerical Methods. In J.-P. Françoise, G.L. Naber and S.T. Tsou (eds.) *Encyclopedia of Mathematical Physics* vol. **2**, pp. 365–374 (2006). Oxford: Elsevier. (ISBN 978-0-1251-2666-3)

Jean-Luc Guermond, LIMSI, CNRS, University Paris Sud, Orsay, France and Texas A&M University, College Station, Texas

The objective of this article is to give an overview of some advanced numerical methods commonly used in fluid mechanics. The focus is set primarily on finite elements methods and finite volume methods.

1. Fluid Mechanics Models

Let Ω be a domain in $\mathbb{R}^d$ ($d = 2, 3$) with boundary $\partial\Omega$ and outer unit normal $\boldsymbol{n}$. Ω is assumed to be occupied by a fluid. The basic equations governing fluid flows are derived from three conservation principles: *conservation of mass, momentum, and energy*. Denoting the density by ρ, the velocity by $\boldsymbol{u}$, and the mass specific internal energy by e_i, these equations are

$$\partial_t\rho + \nabla\cdot(\rho\boldsymbol{u}) = 0 \tag{1}$$

$$\partial_t(\rho\boldsymbol{u}) + \nabla\cdot(\rho\boldsymbol{u}\otimes\boldsymbol{u}) = \nabla\cdot\boldsymbol{\sigma} + \rho\boldsymbol{f}, \tag{2}$$

$$\partial_t(\rho e_i) + \nabla\cdot(\rho\boldsymbol{u}e_i) = \boldsymbol{\sigma}:\boldsymbol{\epsilon} + q_T - \nabla\cdot\boldsymbol{j}_T, \tag{3}$$

where $\boldsymbol{\sigma}$ is the *stress tensor*, $\boldsymbol{\epsilon} = \frac{1}{2}(\nabla\boldsymbol{u} + \nabla\boldsymbol{u})^T$ is the *strain tensor*, $\boldsymbol{f}$ is a body force per unit mass (gravity is a typical example), q_T is a volume source (it may model chemical reactions, Joule effects, radioactive decay, etc.), and $\boldsymbol{j}_T$ is the heat flux. In addition to the above three fundamental conservation equations, one may also have to add L equations that accounts for the conservation of other quantities, say ϕ_ℓ, $1 \le \ell \le L$. These quantities may be the concentration of constituents in an alloy, the turbulent kinetic energy, the mass fractions of various chemical species by unit volume, etc. All these conservation equations take the following form

$$\partial_t(\rho\phi_\ell)+\nabla\cdot(\rho\boldsymbol{u}\phi_\ell) = q_{\phi_\ell}-\nabla\cdot\boldsymbol{j}_{\phi_\ell}, \quad 1 \le \ell \le L. \tag{4}$$

Henceforth the index ℓ is dropped to alleviate the notation.

The above set of equations must be supplemented with initial and boundary conditions. Typical initial conditions are $\rho_{|t=0} = \rho_0$, $\boldsymbol{u}_{|t=0} = \boldsymbol{u}_0$, and $\phi_{|t=0} = \phi_0$. Boundary conditions are usually classified into two types: the *essential boundary conditions* and the *natural boundary conditions*. Natural conditions impose fluxes at the boundary. Typical examples are

$$(\boldsymbol{\sigma}\cdot\boldsymbol{n} + \mathcal{R}\cdot\boldsymbol{u})_{|\partial\Omega} = \boldsymbol{a}_{\boldsymbol{u}},$$

$$(\boldsymbol{j}_T\cdot\boldsymbol{n} + r_T e_i)_{|\partial\Omega} = a_T$$

and

$$(\boldsymbol{j}_\phi\cdot\boldsymbol{n} + r_\phi\phi)_{|\partial\Omega} = a_\phi.$$

The quantities $\mathcal{R}$, r_T, r_ϕ, $\boldsymbol{a}_{\boldsymbol{u}}$, a_T, a_ϕ are given. Essential boundary conditions consist of enforcing boundary values on the dependent variables. One typical example is the so-called *no-slip boundary condition*: $\boldsymbol{u}_{|\partial\Omega} = \boldsymbol{0}$.

The above system of conservation laws is closed by adding three constitutive equations whose purpose is to relate each field $\boldsymbol{\sigma}$, $\boldsymbol{j}_T$, $\boldsymbol{j}_\phi$ to the fields ρ, $\boldsymbol{u}$, and ϕ. They account for microscopic properties of the fluid and thus must be frame independent.

Depending on the constitutive equations and adequate hypotheses on time and space scales, various models are obtained. An important class of fluid model is one for which the stress tensor is a linear function of the strain tensor, yielding the so-called Newtonian fluid model:

$$\boldsymbol{\sigma} = (-p + \lambda \nabla\cdot\boldsymbol{u})\boldsymbol{I} + 2\mu\boldsymbol{\epsilon}. \tag{5}$$

Here p is the pressure, $\boldsymbol{I}$ is the identity matrix, and λ and μ are viscosity coefficients. Still assuming linearity, common models for heat and solute fluxes consist of assuming

$$\boldsymbol{j}_T = -\kappa\nabla T, \qquad \boldsymbol{j}_\phi = -D\nabla\phi, \tag{6}$$

where T is the temperature. These are the so-called Fourier's law and Fick's law, respectively.

Having introduced two new quantities, namely the pressure p and the temperature T, two new scalar relations are needed to close the system. These are the state equations. One admissible assumption consists of setting $\rho = \rho(p, T)$. Another usual additional hypothesis consists of assuming that the variations on the internal energy are proportional to those on the temperature, i.e., $\partial e_i = c_P \partial T$.

Let us now simplify the above models by assuming that ρ is constant. Then, mass conservation implies that the flow is incompressible, i.e., $\nabla\cdot\boldsymbol{u} = 0$. Let us further assume that neither λ, μ, nor p depend on e_i. Then, upon abusing the notation and still denoting by p the ratio p/ρ, the above set of assumptions yields the so-called incompressible Navier–Stokes equations:

$$\nabla\cdot\boldsymbol{u} = 0, \tag{7}$$

$$\partial_t\boldsymbol{u} + \boldsymbol{u}\cdot\nabla\boldsymbol{u} - \nu\Delta\boldsymbol{u} + \nabla p = \boldsymbol{f}. \tag{8}$$

As a result, the mass and momentum conservation equations are independent of that of the energy and those of the solutes:

$$\rho c_P(\partial_t T + \boldsymbol{u}\cdot\nabla T) - \nabla\cdot(\kappa\nabla T) = 2\mu\boldsymbol{\epsilon}:\boldsymbol{\epsilon} + q_T, \tag{9}$$

$$\partial_t\phi + \boldsymbol{u}\cdot\nabla\phi - \tfrac{1}{\rho}\nabla\cdot(D\nabla\phi) = \tfrac{1}{\rho}q_\phi. \tag{10}$$

Another model allowing for a weak dependency of ρ on the temperature, while still enforcing incompressibility, consists of setting $\rho = \rho_0(1-\beta(T-T_0))$. If buoyancy effects induced by gravity are important, it is then possible to account for those by setting $\boldsymbol{f} = \rho_0 g(1 - \beta(T - T_0))$, where g is the gravity acceleration, yielding the so-called Boussinesq model.

Variations on these themes are numerous and a wide range of fluids can be modeled by using nonlinear constitutive laws and nonlinear state laws. For the purpose of numerical simulations, however, it is important to focus on simplified models.

2. The Building Blocks

From the above considerations we now extract a small set of elementary problems which constitute the building blocks of most numerical methods in fluid mechanics.

2.1. Elliptic equations.

By taking the divergence of the momentum equation (8) and assuming $\boldsymbol{u}$ to be known and renaming p to ϕ, one obtains the Poisson equation

$$-\Delta\phi = f, \tag{11}$$

where f is a given source term. This equation plays a key role in the computation of the pressure when solving the Navier–Stokes equations; see (54b). Assuming adequate boundary conditions are enforced, this model equation is the prototype for the class of the so-called elliptic equations. A simple generalization of the Poisson equation consists of the advection-diffusion equation

$$\boldsymbol{u}\cdot\nabla\phi - \nabla\cdot(\kappa\nabla\phi) = f, \tag{12}$$

where $\kappa > 0$. Admissible boundary conditions are $(\kappa\partial_n\phi + r\phi)_{|\partial\Omega} = a$, $r \geq 0$, or $\phi_{|\partial\Omega} = a$. This type of equation is obtained by neglecting the time derivative in the heat equation (9) or in the solute conservation equation (10). Mathematically speaking (12) is also elliptic since its properties (in particular, the way the boundary conditions must be enforced) are controlled by the second-order derivatives. For the sake of simplicity, assume that $\boldsymbol{u} = \boldsymbol{0}$ in the above equation and that the boundary condition is $\phi_{|\partial\Omega} = 0$, then it is possible to show that ϕ solves (12) if and only if ϕ minimizes the following functional

$$\mathcal{J}(\psi) = \int_\Omega (|\nabla\psi|^2 - f\psi)\,\mathrm{d}\boldsymbol{x},$$

where $|\cdot|$ is the Euclidean norm and ψ spans

$$H = \{\psi;\ \textstyle\int_\Omega |\nabla\psi|^2\,\mathrm{d}\boldsymbol{x} < \infty;\ \psi_{|\partial\Omega} = 0\} \tag{13}$$

Writing the first-order optimality condition for this optimization problem yields $\int_\Omega \nabla\phi\cdot\nabla\psi = \int_\Omega f\psi$,

for all $\psi \in H$. This is the so-called variational formulation of (12). When $\boldsymbol{u}$ is not zero, no variational principle holds but a similar way to reformulate (12) consists of multiplying the equation by arbitrary functions in H and integrating by parts the second-order term to give

$$(14)\quad \int_\Omega (\boldsymbol{u}\cdot\nabla\phi)\psi + \kappa\nabla\phi\cdot\nabla\psi = \int_\Omega f\psi, \quad \forall\psi \in H.$$

This is the so-called weak formulation of (12). Weak and variational formulations are the starting point for finite element approximations.

2.2. **Stokes equations.** Another elementary building block is deduced from (8) by assuming that the time derivative and the nonlinear term are both small. The corresponding model is the so-called Stokes equations

$$(15)\qquad -\nu\Delta\boldsymbol{u} + \nabla p = \boldsymbol{f},$$

$$(16)\qquad \nabla\cdot\boldsymbol{u} = 0.$$

Assume for the sake of simplicity that the no-slip boundary condition is enforced: $\boldsymbol{u}_{|\partial\Omega} = \boldsymbol{0}$. Introduce the Lagrangian functional

$$\mathcal{L}(\boldsymbol{v}, q) = \int_\Omega (\nabla\boldsymbol{u}{:}\nabla\boldsymbol{v} - q\nabla\cdot\boldsymbol{v} - \boldsymbol{f}\cdot\boldsymbol{v})\,\mathrm{d}\boldsymbol{x}.$$

Set

$$\boldsymbol{X} = \{\boldsymbol{v};\ \int_\Omega |\nabla\boldsymbol{v}|^2\,\mathrm{d}\boldsymbol{x} < \infty;\ \boldsymbol{v}_{|\partial\Omega} = 0\}$$

$$M = \{q;\ \int_\Omega q^2\,\mathrm{d}\boldsymbol{x} < \infty\}.$$

Then, the pair $(\boldsymbol{u}, p) \in \boldsymbol{X}\times M$ solves the Stokes equations if and only if it is a saddle-point of $\mathcal{L}$, i.e.,

$$(17)\quad \mathcal{L}(\boldsymbol{u}, q) \le \mathcal{L}(\boldsymbol{u}, p) \le \mathcal{L}(\boldsymbol{v}, p), \quad \forall(\boldsymbol{v}, q)\in\boldsymbol{X}\times M.$$

In other words, the pressure p is the Lagrange multiplier of the incompressibility constraint $\nabla\cdot\boldsymbol{u} = 0$. Realizing this fact helps to understand the nature of the Stokes equations, specially when it comes to construct discrete approximations. A variational formulation of the Stokes equations is obtained by writing the first-order optimality condition, namely:

$$\int_\Omega (\nu\nabla\boldsymbol{u}{:}\nabla\boldsymbol{v} - p\nabla\cdot\boldsymbol{v} - \boldsymbol{f}\cdot\boldsymbol{v})\,\mathrm{d}\boldsymbol{x} = 0, \quad \forall\boldsymbol{v} \in \boldsymbol{X},$$

$$\int_\Omega q\nabla\cdot\boldsymbol{u}\,\mathrm{d}\boldsymbol{x} = 0, \quad \forall q \in M.$$

When the nonlinear term is not zero in the momentum equation, or when this term is linearized, there is no saddle-point, but a weak formulation is obtained by multiplying the momentum equation by arbitrary functions $\boldsymbol{v}$ in $\boldsymbol{X}$ and integrating by parts the Laplacian, and by multiplying the mass equation by arbitrary functions q in M:

$$(18)\quad \int_\Omega ((\boldsymbol{u}\cdot\nabla\boldsymbol{u})\cdot\boldsymbol{v} + \nu\nabla\boldsymbol{u}{:}\nabla\boldsymbol{v} - p\nabla\cdot\boldsymbol{v})\,\mathrm{d}\boldsymbol{x} = \int_\Omega \boldsymbol{f}\cdot\boldsymbol{v},$$

$$(19)\quad \int_\Omega q\nabla\cdot\boldsymbol{u} = 0.$$

2.3. **Parabolic equations.** The class of elliptic equations generalizes to that of the parabolic equations when time is accounted for:

$$(20)\quad \partial_t\phi + \boldsymbol{u}\cdot\nabla\phi - \nabla\cdot(\kappa\nabla\phi) = f, \quad \phi_{|t=0} = \phi_0.$$

Fundamentally, this equation has many similarities with the elliptic equation

$$(21)\qquad \alpha\phi + \boldsymbol{u}\cdot\nabla\phi - \nabla\cdot(\kappa\nabla\phi) = f,$$

where $\alpha > 0$. In particular, the set of boundary conditions that are admissible for (20) and (21) are identical, i.e., it is legitimate to enforce $(\kappa\partial_n\phi + r\phi)_{|\partial\Omega} = a$, $r \ge 0$, or $\phi_{|\partial\Omega} = a$. Moreover, solving (21) is always a building block of any algorithm solving (20). The important fact to remember here is that if a good approximation technique for solving (21) is at hand, then extending it to solve (20) is usually straightforward.

2.4. **Hyperbolic equations.** When $\frac{\kappa}{UL} \to 0$, where U is the reference velocity scale and L is the reference length scale, (20) degenerates into the so-called transport equation

$$(22)\qquad \partial_t\phi + \boldsymbol{u}\cdot\nabla\phi = f.$$

This is the prototypical example for the class of hyperbolic equations. For this equation to be well-posed it is necessary to enforce an initial condition $\phi_{|t=0} = \phi_0$ and an inflow boundary condition, i.e., $\phi_{|\partial\Omega^-} = a$, where $\partial\Omega^- = \{\boldsymbol{x} \in \partial\Omega;\ (\boldsymbol{u}\cdot\boldsymbol{n})(\boldsymbol{x}) < 0\}$ is the so-called *inflow boundary* of the domain. To better understand the nature of this equation, introduce the characteristic lines $\boldsymbol{X}(x, s; t)$ of $\boldsymbol{u}(\boldsymbol{x}, t)$ defined as follows:

$$(23)\qquad \begin{cases} d_t\boldsymbol{X}(x, s; t) = \boldsymbol{u}(\boldsymbol{X}(x, s; t), t), \\ \boldsymbol{X}(x, s; s) = \boldsymbol{x}. \end{cases}$$

If $\boldsymbol{u}$ is continuous with respect to t and Lipschitz with respect to $\boldsymbol{x}$, this ODE has a unique solution.

Furthermore, (22) becomes

$$d_t\big[\phi(\boldsymbol{X}(\boldsymbol{x},s;t),t)\big] = f(\boldsymbol{X}(\boldsymbol{x},s;t),t). \tag{24}$$

Then

$$\phi(\boldsymbol{x},t) = \phi_0(\boldsymbol{X}(\boldsymbol{x},t;0)) + \int_0^t f(\boldsymbol{X}(\boldsymbol{x},t;\tau),\tau)\,\mathrm{d}\tau$$

provided $\boldsymbol{X}(\boldsymbol{x},t;\tau) \in \Omega$ for all $\tau \in [0,t]$. This shows that the concept of characteristic curves is important to construct an approximation to (22).

3. Meshes

The starting point of every approximation technique for solving any of the above model problems consists of defining a mesh of Ω on which the approximate solution is defined. To avoid having to account for curved boundaries, let us assume the domain Ω is a two-dimensional polygon (resp. three-dimensional polyhedron). A mesh of Ω, say $\mathcal{T}_h$, is a partition of Ω into small cells hereafter assumed to be simple convex polygons in two dimensions (resp. polyhedrons in three dimensions), say triangles or quadrangles (resp. tetrahedrons or cuboids). Moreover, this partition is usually assumed to be such that if two different cells have a nonempty intersection, then the intersection is a vertex, or an entire edge, or an entire face. The left panel of Figure 1 shows a mesh satisfying the above requirement. The mesh in the right panel is not admissible.

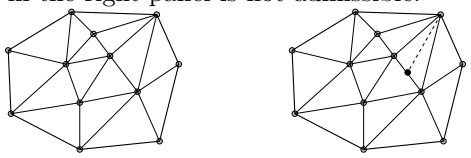

Fig 1: *Admissible (left) and nonadmissible (right) meshes.*

4. Finite Elements: Interpolation

The finite element method is foremost an interpolation technique. The goal of this section is to illustrate this idea by giving examples.

Let $\mathcal{T}_h = \{K_m\}_{1\le m\le N_{\mathrm{el}}}$ be a mesh composed of N_{el} simplices, i.e., triangles in two dimensions or tetrahedrons in three dimensions. Consider the following vector spaces of functions

$$V_h = \{v_h \in \mathcal{C}^0(\overline{\Omega});\, v_{h|K_m} \in \mathbb{P}_k,\ 1 \le m \le N_{\mathrm{el}}\}, \tag{25}$$

where $\mathbb{P}_k$ denotes the space of polynomials of global degree at most k. V_h is called a *finite element approximation space*. We now construct a basis for V_h.

Given a simplex K_m in $\mathbb{R}^d$, let $\boldsymbol{v}_n$ be a vertex of K_m, let F_n be the face of K_m opposite to $\boldsymbol{v}_n$, and define $\boldsymbol{n}_n$ to be the outward normal to F_n, $1 \le n \le d+1$. Define the *barycentric coordinates*

$$\lambda_n(\boldsymbol{x}) = 1 - \frac{(\boldsymbol{x}-\boldsymbol{v}_n)\cdot\boldsymbol{n}_n}{(\boldsymbol{v}_l-\boldsymbol{v}_n)\cdot\boldsymbol{n}_n}, \quad 1 \le n \le d+1, \tag{26}$$

where $\boldsymbol{v}_l$ is an arbitrary vertex in F_n (the definition of λ_n is clearly independent of $\boldsymbol{v}_l$ provided $\boldsymbol{v}_l$ belongs to F_n). The barycentric coordinate λ_n is an affine function; it is equal to 1 at $\boldsymbol{v}_n$ and vanishes on F_n; its level-sets are hyperplanes parallel to F_n. The barycenter of K_m has barycentric coordinates

$$(\frac{1}{d+1},\dots,\frac{1}{d+1}).$$

The barycentric coordinates satisfy the following properties: For all $\boldsymbol{x} \in K_m$, $0 \le \lambda_n(\boldsymbol{x}) \le 1$, and for all $\boldsymbol{x} \in \mathbb{R}^d$,

$$\sum_{n=1}^{d+1} \lambda_n(\boldsymbol{x}) = 1, \quad \text{and} \quad \sum_{n=1}^{d+1} \lambda_n(\boldsymbol{x})(\boldsymbol{x}-\boldsymbol{v}_n) = 0.$$

Consider the set of nodes $\{\boldsymbol{a}_{n,m}\}_{1\le n\le n_{\mathrm{sh}}}$ of K_m with barycentric coordinates

$$\left(\frac{i_0}{k},\dots,\frac{i_d}{k}\right), \quad 0 \le i_0,\dots,i_d \le k,\ i_0+\ldots+i_d = k.$$

These points are called the *Lagrange nodes* of K_m. It is clear that there are $n_{\mathrm{sh}} = \frac{1}{2}(k+1)(k+2)$ of these points in two dimensions and $n_{\mathrm{sh}} = \frac{1}{6}(k+1)(k+2)(k+3)$ in three dimensions. It is remarkable that $n_{\mathrm{sh}} = \dim \mathbb{P}_k$.

Let $\{\boldsymbol{b}_1,\dots,\boldsymbol{b}_N\} = \bigcup_{K_m\in\mathcal{T}_h}\{\boldsymbol{a}_{1,m},\dots,\boldsymbol{a}_{n_{\mathrm{sh}},m}\}$ be the set of all the Lagrange nodes in the mesh. For $K_m \in \mathcal{T}_h$ and $n \in \{1,\dots,n_{\mathrm{sh}}\}$, let $j(n,m) \in \{1,\dots,N\}$ be the integer such that $\boldsymbol{a}_{n,m} = \boldsymbol{b}_{j(n,m)}$; $j(n,m)$ is the global index of the Lagrange node $\boldsymbol{a}_{n,m}$. Let $\{\varphi_1,\dots,\varphi_N\}$ be the set of functions in V_h defined by $\varphi_i(\boldsymbol{b}_j) = \delta_{ij}$, then it can be shown that

$$\{\varphi_1,\dots,\varphi_N\} \text{ is a basis for } V_h. \tag{27}$$

The functions φ_i are called *global shape functions*. An important property of global shape functions is that their supports are small sets of cells. More precisely, let $i \in \{1,\dots N\}$ and let $\mathcal{V}_i = \{m;\, \exists n;\, i = j(n,m)\}$ be the set of cell indices to which the node

$\boldsymbol{b}_i$ belongs, then the support of φ_i is $\cup_{m\in\mathcal{V}_i} K_m$. For $k=1$, it is clear that $\varphi_{i|K_m} = \lambda_n$ for all $m \in \mathcal{V}_i$ and all n such that $i = j(n,m)$, and $\varphi_{i|K_m} = 0$ otherwise. The graph of such a shape function in two dimensions is shown in the left panel of Figure 2. For $k=2$, enumerate from 1 to $d+1$ the vertices of K_m, and enumerate from $d+2$ to $n_{\rm sh}$ the Lagrange nodes located at the midedges. For a midedge node of index $d+2 \le n \le n_{\rm sh}$, let $b(n), e(n) \in \{1,\dots,d+1\}$ be the two indices of the two Lagrange nodes at the extremities of the edge in question. Then, the restriction to K_m of a $\mathbb{P}_2$ shape function φ_i is

$$\varphi_{i|K_m} = \begin{cases} \lambda_n(2\lambda_n - 1), & \text{if } 1 \le n \le d+1, \\ 4\lambda_{b(n)}\lambda_{e(n)}, & \text{if } d+2 \le n \le n_{\rm sh}, \end{cases} \tag{28}$$

Figure 2 shows the graph of two $\mathbb{P}_2$ shape functions in two dimensions.

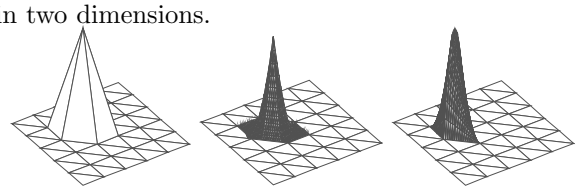

Fig 2: *Two-dimensional Lagrange shape functions: Piecewise $\mathbb{P}_1$ (left) and Piecewise $\mathbb{P}_2$ (center and right).*

Once the space V_h is introduced, it is natural to define the interpolation operator

$$\Pi_h : \mathcal{C}^0(\overline{\Omega}) \ni v \longmapsto \sum_{i=1}^{N} v(\boldsymbol{b}_i)\varphi_i \in V_h. \tag{29}$$

This operator is such that for all continuous function v, the restriction of $\Pi_h(v)$ to each mesh cell is a polynomial in $\mathbb{P}_k$ and $\Pi_h(v)$ takes the same values as v at the Lagrange nodes. Moreover, setting $h = \max_{K_m\in\mathcal{T}_h} \mathrm{diam}(K_m)$, and defining

$$\|r\|_{L^p} = \Big(\int_\Omega |r|^p \,\mathrm{d}\boldsymbol{x}\Big)^{\frac{1}{p}} \quad \text{for } 1 \le p < \infty,$$

the following approximation result holds

$$\|v - \Pi_h(v)\|_{L^p} + h\|\nabla(v - \Pi_h(v))\|_{L^p} \le ch^{k+1}\|v\|_{\mathcal{C}^{k+1}(\overline{\Omega})}, \tag{30}$$

where c is a constant that depends on the quality of the mesh. More precisely, for $K_m \in \mathcal{T}_h$, let ρ_{K_m} be the diameter of the largest ball that can be inscribed into K_m and let h_{K_m} be the diameter of K_m. Then, c depends on $\sigma = \max_{K_m\in\mathcal{T}_h} h_{K_m}/\rho_{K_m}$. Hence, for the mesh to have good interpolation properties, it is recommended that the cells be not too flat. Families of meshes for which σ is bounded uniformly with respect to h as $h \to 0$ are said to be *shape-regular families*.

The above example of finite element approximation space generalizes easily to meshes composed of quadrangles or cuboids. In this case, the shape functions are piecewise polynomial of partial degree at most k. These spaces are usually referred to as $\mathbb{Q}_k$ approximation spaces.

5. Finite Elements: Approximation

We show in this section how finite element approximation spaces can be used to approximate some model problems exhibited in §2.

5.1. Advection-diffusion.

Consider the model problem (21) supplemented with the boundary condition $(\kappa\partial_n\phi + r\phi)_{|\partial\Omega} = g$. Assume $\kappa > 0$, $\alpha + \frac{1}{2}\nabla\cdot\boldsymbol{u} \ge 0$, and $r \ge 0$. Define

$$a(\phi,\psi) = \int_\Omega ((\alpha\phi + \beta\cdot\nabla\phi)\psi + \kappa\nabla\phi\cdot\nabla\psi)\,\mathrm{d}\boldsymbol{x} + \int_{\partial\Omega} r\phi\psi\,\mathrm{d}s.$$

Then, the weak formulation of (21) is: Seek $\phi \in H$ (H defined in (13)) such that for all $\psi \in H$

$$a(\phi,\psi) = \int_\Omega f\psi\,\mathrm{d}\boldsymbol{x} + \int_{\partial\Omega} g\psi\,\mathrm{d}s. \tag{31}$$

Using the approximation space V_h defined in (25) together with the basis defined in (27), we seek an approximate solution to the above problem in the form $\phi_h = \sum_{i=1}^N U_i\varphi_i \in V_h$. Then, a simple way of approximating (31) consists of seeking $U = (U_1,\dots,U_N)^T \in \mathbb{R}^N$ such that for all $1 \le i \le N$

$$a(\phi_h,\varphi_i) = \int_\Omega f\varphi_i\,\mathrm{d}\boldsymbol{x} + \int_{\partial\Omega} g\varphi_i\,\mathrm{d}s. \tag{32}$$

This problem finally amounts to solving the following linear system

$$\mathcal{A}U = F, \tag{33}$$

where $\mathcal{A}_{ij} = a(\varphi_j,\varphi_i)$ and $F_i = \int_\Omega f\varphi_i\,\mathrm{d}\boldsymbol{x} + \int_{\partial\Omega} g\varphi_i\,\mathrm{d}s$. The above approximation technique is usually referred to as *the Galerkin method*. The following error estimate can be proved

$$\|\phi - \phi_h\|_{L^p} + h\|\nabla(\phi - \phi_h)\|_{L^p} \le ch^{k+1}\|\phi\|_{\mathcal{C}^{k+1}(\overline{\Omega})}, \tag{34}$$

where in addition to depending on the shape-regularity of the mesh, the constant c also depends on κ, α, and β.

5.2. **Stokes equations.** The line of thought developed above can be used to approximate the Navier–Stokes problem (15)–(16). Let us assume that the nonlinear term $\boldsymbol{u}\cdot\nabla\boldsymbol{u}$ is linearized in the form $\boldsymbol{v}\cdot\nabla\boldsymbol{u}$, where $\boldsymbol{v}$ is known. Let $\mathcal{T}_h$ be a mesh of Ω, and assume that finite element approximation spaces have been constructed to approximate the velocity and the pressure, say $\boldsymbol{X}_h$ and M_h. Assume for the sake of simplicity that $\boldsymbol{X}_h \subset \boldsymbol{X}$ and $M_h \subset M$. Assume that bases for $\boldsymbol{X}_h$ and M_h are at hand, say $\{\boldsymbol{\varphi}_1,\dots,\boldsymbol{\varphi}_{N_u}\}$ and $\{\psi_1,\dots,\psi_{N_p}\}$, respectively. Set

$$a(\boldsymbol{u},\boldsymbol{\varphi}) = \int_\Omega ((\boldsymbol{v}\cdot\nabla\boldsymbol{u})\cdot\boldsymbol{\varphi} + \nu\nabla\boldsymbol{u}{:}\nabla\boldsymbol{\varphi}\,\mathrm{d}\boldsymbol{x}$$

and

$$b(\boldsymbol{v},\psi) = -\int_\Omega \psi\nabla\cdot\boldsymbol{v}\,\mathrm{d}\boldsymbol{x}.$$

Then, we seek an approximate velocity $\boldsymbol{u}_h = \sum_{i=1}^{N_u} U_i\boldsymbol{\varphi}_i$ and an approximate pressure $p_h = \sum_{k=1}^{N_p} P_k\psi_k$ such that for all $i \in \{1,\dots,N_u\}$ and all $k \in \{1,\dots,N_p\}$ the following holds

$$a(\boldsymbol{u}_h,\boldsymbol{\varphi}_i) + b(\boldsymbol{\varphi}_i,p_h) = \int_\Omega \boldsymbol{f}\cdot\boldsymbol{\varphi}_i\,\mathrm{d}\boldsymbol{x}, \tag{35}$$

$$b(\boldsymbol{u}_h,\psi_k) = 0. \tag{36}$$

Define the matrix $\mathcal{A} \in \mathbb{R}^{N_u,N_u}$ such that $\mathcal{A}_{ij} = a(\boldsymbol{\varphi}_j,\boldsymbol{\varphi}_i)$. Define the matrix $\mathcal{B} \in \mathbb{R}^{N_p,N_u}$ such that $\mathcal{B}_{ki} = b(\boldsymbol{\varphi}_i,\psi_k)$. Then, the above problem can be recast into the following partitioned linear system

$$\left[\begin{array}{c:c} \mathcal{A} & \mathcal{B}^T \\ \hdashline \mathcal{B} & 0 \end{array}\right] \begin{bmatrix} U \\ P \end{bmatrix} = \begin{bmatrix} F \\ 0 \end{bmatrix}, \tag{37}$$

where the vector $F \in \mathbb{R}^{N_u}$ is such that $F_i = \int_\Omega \boldsymbol{f}\cdot\boldsymbol{\varphi}_i$.

An important aspect of the above approximation technique is that for the linear system to be invertible, the matrix $\mathcal{B}^T$ must have full row rank (i.e., $\mathcal{B}$ has full column rank). This amounts to

$$\exists\beta_h > 0, \quad \inf_{q_h\in M_h}\sup_{\boldsymbol{v}_h\in\boldsymbol{X}_h} \frac{\int_\Omega q_h\nabla\cdot\boldsymbol{v}_h\,\mathrm{d}\boldsymbol{x}}{\|\boldsymbol{v}_h\|_X\|q_h\|_M} \ge \beta_h, \tag{38}$$

where

$$\|\boldsymbol{v}_h\|_X^2 = \int_\Omega |\nabla\boldsymbol{v}_h|^2\,\mathrm{d}\boldsymbol{x}, \qquad \|q_h\|_M^2 = \int_\Omega q_h^2\,\mathrm{d}\boldsymbol{x}.$$

This nontrivial condition is called the *Ladyženskaja–Babuška–Brezzi condition* (LBB) in the literature. For instance, if $\mathbb{P}_1$ finite elements are used to approximate both the velocity and the pressure, the above condition does not hold, since there are nonzero pressure fields q_h in M_h such that $\int_\Omega q_h\nabla\cdot\boldsymbol{v}_h\,\mathrm{d}\boldsymbol{x} = 0$ for all $\boldsymbol{v}_h$ in $\boldsymbol{X}_h$. Such fields are called *spurious pressure modes*. An example is shown in Figure 3. The spurious function alternatively takes the values -1, 0, and $+1$ at the vertices of the mesh so that its mean value on each cell is zero.

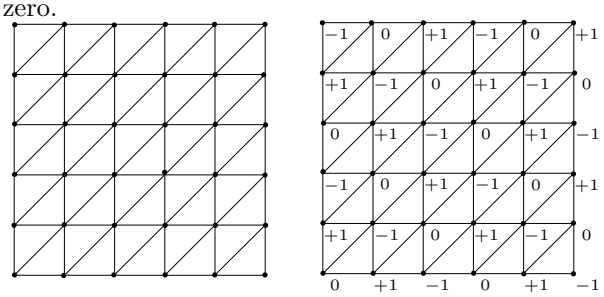

Fig 3: *The $\mathbb{P}_1/\mathbb{P}_1$ finite element: the mesh (left); one pressure spurious mode (right).*

Couples of finite element spaces satisfying the LBB condition are numerous. For instance, assuming $k \ge 2$, using $\mathbb{P}_k$ finite elements to approximate the velocity and $\mathbb{P}_{k-1}$ finite elements to approximate the pressure is acceptable. Likewise using $\mathbb{Q}_k$ elements for the velocity and $\mathbb{Q}_{k-1}$ elements for the pressure on meshes composed of quadrangles or cuboids is admissible.

Approximation techniques for which the pressure and the velocity degrees of freedom are not associated with the same nodes are usually called *staggered approximations*. Staggering pressure and velocity unknowns is common in solution methods for the incompressible Stokes and Navier–Stokes equations; see also §7.3.

6. Finite Volumes: Principles

The finite volume method is an approximation technique whose primary goal is to approximate conservation equations, whether time-dependent or not. Given a mesh, say $\mathcal{T}_h = \{K_m\}_{1\le m\le N_{\mathrm{el}}}$, and a conservation equation

$$\alpha\partial_t\phi + \nabla\cdot\boldsymbol{F}(\phi,\nabla\phi,\boldsymbol{x},t) = f, \tag{39}$$

($\alpha = 0$ if the problem is time-independent and $\alpha = 1$ otherwise), the main idea underlying every finite volume method is to represent the approximate solution by its mean values over the mesh

cells $(\phi_{K_1},\dots,\phi_{K_{N_{\rm el}}})^T \in \mathbb{R}^{N_{\rm el}}$ and to test the conservation equation by the characteristic functions of the mesh cells $\{1_{K_1},\dots,1_{K_{N_{\rm el}}}\}$. For each cell $K_m \in \mathcal{T}_h$, denote by $\boldsymbol{n}_{K_m}$ the outward unit normal vector and denote by $\mathcal{F}_m$ the set of the faces of K_m. The finite volume approximation to (39) consists of seeking $(\phi_{K_1},\dots,\phi_{K_{N_{\rm el}}})^T \in \mathbb{R}^{N_{\rm el}}$ such that the function $\phi_h = \sum_{m=1}^{N_{\rm el}} \phi_{K_m} 1_{K_1 m}$ satisfies the following: For all $1 \le m \le N_{\rm el}$

$$|K_m|\alpha d_t \phi_{K_m}(t) + \sum_{\sigma\in\mathcal{F}_m} F_h^{m,\sigma}(\phi_h,\nabla_h\phi_h,t) = \int_K f\,\mathrm{d}\boldsymbol{x}, \tag{40}$$

where

$$|K_m| = \int_K \mathrm{d}\boldsymbol{x},$$

$\nabla_h\phi_h$ is an approximation of $\nabla\phi$, and $F_h^{m,\sigma}$ is an approximation of

$$\int_\sigma \boldsymbol{F}(\phi,\nabla\phi,\boldsymbol{x},t)\cdot\boldsymbol{n}_{K_m}\,\mathrm{d}\boldsymbol{\sigma}.$$

The precise definition of the so-called approximate flux $F_h^{m,\sigma}$ depends on the the nature of the problem (e.g., elliptic, parabolic, hyperbolic, saddle point) and the desired accuracy. In general the approximate fluxes are required to satisfy the following two important properties:

1. *Conservativity*: For $K_m, K_l \in \mathcal{T}_h$ such that $\sigma = K_m \cap K_l$, $F_h^{m,\sigma} = -F_h^{l,\sigma}$.
2. *Consistency*: Let ψ be the solution to (39), and set $\psi_h = \frac{1_{K_1}}{|K_1|}\int_{K_1}\psi\,\mathrm{d}\boldsymbol{x} + \ldots + \frac{1_{K_{N_{\rm el}}}}{|K_{N_{\rm el}}|}\int_{K_{N_{\rm el}}}\psi\,\mathrm{d}\boldsymbol{x}$, then

$$F_h^{m,\sigma}(\psi_h,\nabla_h\psi_h,t) \xrightarrow{h\to 0} \int_\sigma \boldsymbol{F}(\psi,\nabla\psi,\boldsymbol{x},t)\cdot\boldsymbol{n}\,\mathrm{d}\boldsymbol{\sigma}.$$

The quantity

$$|F_h^{m,\sigma}(\psi_h,\nabla_h\psi_h,t) - \int_\sigma \boldsymbol{F}(\psi,\nabla\psi,\boldsymbol{x},t)\cdot\boldsymbol{n}\,\mathrm{d}\boldsymbol{\sigma}|$$

is called the consistency error.

Note that (40) is a system of Ordinary Differential Equations (ODEs). This system is usually discretized in time by using standard time-marching techniques such as explicit Euler, Runge-Kutta, etc.

The discretization technique above described is sometimes referred to as *cell-centered finite volume method*. Another method, called *vertex-centered finite volume*, consists of using the characteristic functions associated with the vertices of the mesh instead of those associated with the cells.

7. Finite Volumes: Examples

In this section we illustrate the ideas introduced above. Three examples are developed: the Poisson equation, the transport equation, and the Stokes equations.

7.1. Poisson problem.

Consider the Poisson equation (11) equipped with the boundary condition $\partial_n\phi_{|\partial\Omega} = a$. To avoid technical details, assume that $\Omega =]0,1[^d$. Let $\mathcal{K}_h$ be a mesh of Ω composed of rectangles (or cuboids in three dimensions).

The flux function is $\boldsymbol{F}(\phi,\nabla\phi,\boldsymbol{x}) = -\nabla\phi$; hence, $F_h^{m,\sigma}$ must be a consistent conservative approximation of $-\int_\sigma \boldsymbol{n}_{K_m}\cdot\nabla\phi\,\mathrm{d}\boldsymbol{\sigma}$. Let σ be an interior face of the mesh and let K_m, K_l be the two cells such that $\sigma = K_m \cap K_l$. Let $\boldsymbol{x}_{K_m}, \boldsymbol{x}_{K_l}$ be the barycenters of K_m and K_l, respectively. Then, an admissible formula for the approximate flux is

$$F_h^{m,\sigma} = -\frac{|\sigma|}{|\boldsymbol{x}_{K_m} - \boldsymbol{x}_{K_l}|}(\phi_{K_l} - \phi_{K_m}), \tag{41}$$

where $|\sigma| = \int_\sigma \mathrm{d}\boldsymbol{\sigma}$. The consistency error is $\mathcal{O}(h)$ in general, and is $\mathcal{O}(h^2)$ if the mesh is composed of identical cuboids. The conservativity is evident. If σ is part of $\partial\Omega$, an admissible formula for the approximate flux is $F_h^{m,\sigma} = -\int_\sigma a\,\mathrm{d}\boldsymbol{\sigma}$. Then, upon defining $\mathcal{F}_{K_m}^i = \mathcal{F}_{K_m}\backslash\partial\Omega$ and $\mathcal{F}_{K_m}^\partial = \mathcal{F}_{K_m}\cap\partial\Omega$, the finite volume approximation of the Poisson problem is: Seek $\phi_h \in \mathbb{R}^{N_{\rm el}}$ such that for all $1 \le m \le N_{\rm el}$

$$\sum_{\sigma\in\mathcal{F}_{K_m}^i} F_h^{m,\sigma} = \int_{K_m} f\,\mathrm{d}\boldsymbol{x} + \sum_{\sigma\in\mathcal{F}_{K_m}^\partial}\int_\sigma a\,\mathrm{d}\boldsymbol{\sigma}. \tag{42}$$

7.2. Transport equation.

Consider the transport equation

$$\partial_t\phi + \nabla\cdot(\boldsymbol{u}\phi) = f, \tag{43}$$

$$\phi_{|t=0} = \phi_0, \quad \phi_{|\partial\Omega^-} = a, \tag{44}$$

where $\boldsymbol{u}(\boldsymbol{x},t)$ is a given field in $\mathcal{C}^1(\overline{\Omega}\times[0,T])$. Let $\mathcal{T}_h$ be a mesh of Ω. For the sake of simplicity, let us use the explicit Euler time-stepping to approximate (40). Let N be positive integer, set $\Delta t = \frac{T}{N}$, set $t^n = n\Delta t$ for $0 \le n \le N$, and partition $[0,T]$ as follows

$$[0,T] = \bigcup_{n=0}^{N-1}[t^n, t^{n+1}].$$

Denote by $\phi_h^n \in \mathbb{R}^{N_{\rm el}}$ the finite volume approximation of $\phi_h(t^n)$. Then, (40) is approximated as follows

$$\frac{|K_m|}{\Delta t}(\phi_{K_m}^{n+1} - \phi_{K_m}^n) + \sum_{\sigma\in\mathcal{F}_m} F_h^{m,\sigma}(\phi_h, \nabla_h\phi_h, t^n) = \int_K f(\boldsymbol{x}, t^n)\,\mathrm{d}\boldsymbol{x}, \tag{45}$$

where $\phi_{K_m}^0 = \int_{K_m}\phi_0\,\mathrm{d}\boldsymbol{x}$. The approximate flux $F_h^{m,\sigma}$ must be a consistent conservative approximation of $\int_\sigma(\boldsymbol{u}\cdot\boldsymbol{n}_{K_m})\phi\,\mathrm{d}\boldsymbol{\sigma}$. Let σ be a face of the mesh and let K_m, K_l be the two cells such that $\sigma = K_m\cap K_l$ (note that if σ is on $\partial\Omega$, σ belongs to one cell only and we set $K_m = K_l$). If σ is on $\partial\Omega^-$, set

$$F_h^{m,\sigma} = \int_\sigma(\boldsymbol{u}\cdot\boldsymbol{n}_{K_m})a\,\mathrm{d}\boldsymbol{\sigma}. \tag{46}$$

If σ is not on $\partial\Omega^-$, set $u_{m,\sigma}^n = \int_\sigma(\boldsymbol{u}\cdot\boldsymbol{n}_{K_m})\,\mathrm{d}\boldsymbol{\sigma}$ and define

$$F_h^{m,\sigma} = \begin{cases}\phi_{K_m}^n u_{m,\sigma}^n & \text{if } u_{m,\sigma}^n \ge 0,\\ \phi_{K_l}^n u_{m,\sigma}^n & \text{if } u_{m,\sigma}^n < 0.\end{cases} \tag{47}$$

The above choice for the approximate flux is usually called the *upwind flux*. It is consistent with the analysis that has been done for (22), i.e., information flows along the characteristic lines of the field $\boldsymbol{u}$; see (24). In other words, the updating of $\phi_{k_m}^{n+1}$ must be done by using the approximate values ϕ_h^n coming from the cells that are upstream the flow field.

An important feature of the above approximation technique is that it is L^∞-stable in the sense that

$$\max_{0\le n\le N, 1\le m\le N_{\rm el}}|\phi_{K_m}^n| \le c(u_0, f)$$

if the two mesh parameters Δt and h satisfy the so-called *Courant–Friedrichs–Levy* (CFL) condition $\|\boldsymbol{u}\|_{L^\infty}\Delta t/h \le c(\sigma)$, where $c(\sigma)$ is a constant that depends on the mesh regularity parameter $\sigma = \max_{K_m\in\mathcal{T}_h} h_{K_m}/\rho_{K_m}$. In one dimension $c(\sigma) = 1$.

7.3. **Stokes equations.** To finish this short review of finite volume methods, we turn our attention to the Stokes problem (15)–(16) equipped with the homogeneous Dirichlet boundary condition $\boldsymbol{u}_{|\partial\Omega} = \boldsymbol{0}$.

Let $\mathcal{T}_h$ be a mesh of Ω composed of triangles (or tetrahedrons). All the angles in the triangulation are assumed to be acute so that for all $K\in\mathcal{T}_h$, the intersection of the orthogonal bisectors of the sides of K, say $\boldsymbol{x}_K$, is in K. We propose a finite volume approximation for the velocity and a finite element approximation for the pressure. Let $\{\boldsymbol{e}_1,\dots,\boldsymbol{e}_d\}$ be a Cartesian basis for $\mathbb{R}^d$. Set $\mathbf{1}_{K_m}^k = 1_{K_m}\boldsymbol{e}_k$ for all $1\le m\le N_{\rm el}$ and $1\le k\le d$, then define

$$\boldsymbol{X}_h = \mathrm{span}\{\mathbf{1}_{K_1}^1,\dots,\mathbf{1}_{K_1}^d,\dots,\mathbf{1}_{K_{N_{\rm el}}}^1,\dots,\mathbf{1}_{K_{N_{\rm el}}}^d\}.$$

Let $\{\boldsymbol{b}_1,\dots,\boldsymbol{b}_{N_{\rm v}}\}$ be the vertices of the mesh, and let $\{\varphi_1,\dots,\varphi_{N_{\rm v}}\}$ be the associated piecewise linear global shape functions. Then, set

$$N_h = \mathrm{span}\{\varphi_1,\dots,\varphi_{N_{\rm v}}\},$$
$$M_h = \{q\in N_h;\ \int_\Omega q\,\mathrm{d}\boldsymbol{x} = 0\};$$

see §4. The approximate problem consists of seeking $(\boldsymbol{u}_{K_1},\dots,\boldsymbol{u}_{K_{N_{\rm el}}})\in\mathbb{R}^{dN_{\rm el}}$ and $p_h\in M_h$ such that for all $1\le m\le N_{\rm el}$, $1\le k\le d$, and all $1\le i\le N_{\rm v}$,

$$\sum_{\sigma\in\mathcal{F}_m}\mathbf{1}_{K_m}^k\cdot\boldsymbol{F}_h^{m,\sigma} + c(\mathbf{1}_{K_m}^k, p_h) = \int_{K_m}\mathbf{1}_{K_m}^k\cdot\boldsymbol{f}\,\mathrm{d}\boldsymbol{x}, \tag{48}$$

$$c(\boldsymbol{u}_{K_m}, \varphi_i) = 0, \tag{49}$$

where

$$c(\boldsymbol{v}_{K_m}, p_h) = \int_{K_m}\boldsymbol{v}_{K_m}\cdot\nabla p_h\,\mathrm{d}\boldsymbol{x}.$$

Moreover,

$$\boldsymbol{F}_h^{m,\sigma} = \begin{cases}\dfrac{\nu|\sigma|}{|\boldsymbol{x}_m - \boldsymbol{x}_l|}(\boldsymbol{u}_{K_m} - \boldsymbol{u}_{K_l}) & \text{if } \sigma = K_m\cap K_l,\\ \dfrac{\nu|\sigma|}{d(\boldsymbol{x}_m,\sigma)}\boldsymbol{u}_{K_m} & \text{if } \sigma = K_m\cap\partial\Omega,\end{cases}$$

where $d(\boldsymbol{x}_{K_m},\sigma)$ is the Euclidean distance between $\boldsymbol{x}_{K_m}$ and σ. This formulation yields a linear system with the same structure as in (37). Note in particular that

$$\sup_{\boldsymbol{v}_h\in\boldsymbol{X}_h}\frac{c(\boldsymbol{v}_h, p_h)}{\|\boldsymbol{v}_h\|_{L^\infty}} = \|\nabla p_h\|_{L^1}, \tag{50}$$

Since the mean-value of p_h is zero, $\|\nabla p_h\|_{L^1}$ is a norm on M_h. As a result, an inequality similar to (38) holds. This inequality is a key step to proving that the linear system is wellposed and the approximate solution converges to the exact solution of (15)–(16).

8. Projection methods for Navier–Stokes

In this section we focus on the time approximation of the Navier–Stokes problem:

$$\partial_t \boldsymbol{u} - \nu\Delta\boldsymbol{u} + \boldsymbol{u}\cdot\nabla\boldsymbol{u} + \nabla p = \boldsymbol{f}, \tag{51a}$$

$$\nabla\cdot\boldsymbol{u} = 0, \tag{51b}$$

$$\boldsymbol{u}_{|\partial\Omega} = 0, \tag{51c}$$

$$\boldsymbol{u}_{|t=0} = \boldsymbol{u}_0. \tag{51d}$$

where $\boldsymbol{f}$ is a body force and $\boldsymbol{u}_0$ is a solenoidal velocity field. There are numerous ways to discretize this problem in time, but, undoubtedly, one of the most popular strategies is to use projection methods, sometimes also referred to as *Chorin–Temam methods*.

A projection method is a fractional-step time-marching technique. It is a predictor–corrector strategy aiming at uncoupling viscous diffusion and incompressibility effects. One time step is composed of three substeps: in the first substep, the pressure is made explicit and a provisional velocity field is computed using the momentum equation; in the second substep, the provisional velocity field is projected onto the space of incompressible (solenoidal) vector fields; in the third substep, the pressure is updated.

Let $q > 0$ be an integer and approximate the time derivative of $\boldsymbol{u}$ using a backward difference formula of order q. To this end, introduce a positive integer N, set $\Delta t = \frac{T}{N}$, set $t^n = n\Delta t$ for $0 \le n \le N$, and consider a partitioning of the time interval in the form

$$[0,T] = \bigcup_{n=0}^{N-1} [t^n, t^{n+1}].$$

For all sequences $\boldsymbol{v}_{\Delta t} = (\boldsymbol{v}^0, \boldsymbol{v}^1, \dots, \boldsymbol{v}^N)$, set

$$D^{(q)}\boldsymbol{v}^{n+1} = \beta_q \boldsymbol{v}^{n+1} - \sum_{j=0}^{q-1} \beta_j \boldsymbol{v}^{n-j}, \tag{52}$$

where $q-1 \le n \le N-1$. The coefficients β_j are such that

$$\frac{1}{\Delta t}(\beta_q \boldsymbol{u}(t^{n+1}) - \sum_{j=0}^{q-1} \beta_j \boldsymbol{u}(t^{n-j}))$$

is a qth-order backward difference formula approximating $\partial_t \boldsymbol{u}(t^{n+1})$. For instance,

$$D^{(1)}\boldsymbol{v}^{n+1} = \boldsymbol{v}^{n+1} - \boldsymbol{v}^n,$$
$$D^{(2)}\boldsymbol{v}^{n+1} = \tfrac{3}{2}\boldsymbol{v}^{n+1} - 2\boldsymbol{v}^n + \tfrac{1}{2}\boldsymbol{v}^{n-1}.$$

Furthermore, for all sequences $\phi_{\Delta t} = (\phi^0, \phi^1, \dots, \phi^N)$, define

$$\phi^{\star,n+1} = \sum_{j=0}^{q-1} \gamma_j \phi^{n-j}, \tag{53}$$

so that $\sum_{j=0}^{q-1} \gamma_j p(t^{n-j})$ is a $(q-1)$th-order extrapolation of $p(t^{n+1})$. For instance, $p^{\star,n+1} = 0$ for $q = 1$, $p^{\star,n+1} = p^n$ for $q = 2$, and $p^{\star,n+1} = 2p^n - p^{n-1}$ for $q = 3$. Finally, denote by $(\boldsymbol{u}\cdot\nabla\boldsymbol{u})^{\star,n+1}$ a q-th order extrapolation of $(\boldsymbol{u}\cdot\nabla\boldsymbol{u})(t^{n+1})$. For instance,

$$(\boldsymbol{u}\cdot\nabla\boldsymbol{u})^{\star,n+1} = \begin{cases} \boldsymbol{u}^n\cdot\nabla\boldsymbol{u}^n & \text{if } q=1, \\ 2\boldsymbol{u}^n\cdot\nabla\boldsymbol{u}^n - \boldsymbol{u}^{n-1}\cdot\nabla\boldsymbol{u}^{n-1} & \text{if } q=2. \end{cases}$$

A general projection algorithm is as follows. Set $\tilde{\boldsymbol{u}}^0 = \boldsymbol{u}_0$ and $\phi^l = 0$ for $0 \le l \le q-1$. If $q > 1$, assume that $\tilde{\boldsymbol{u}}^1, \dots, \tilde{u}^{q-1}$, $p^{\star,q}$ and $(\boldsymbol{u}\cdot\nabla\boldsymbol{u})^{\star,q}$ have been initialized properly. For $n \ge q-1$, seek $\tilde{\boldsymbol{u}}^{n+1}$ such that $\tilde{\boldsymbol{u}}^{n+1}_{|\partial\Omega} = 0$ and

$$\begin{aligned} &\tfrac{D^{(q)}}{\Delta t}\tilde{\boldsymbol{u}}^{n+1} - \nu\Delta\tilde{\boldsymbol{u}}^{n+1} \\ &\quad + \nabla\left(p^{\star,n+1} + \textstyle\sum_{j=0}^{q-1} \frac{\beta_j}{\Delta t}\phi^{n-j}\right) = \boldsymbol{S}^{n+1}, \end{aligned} \tag{54a}$$

where $\boldsymbol{S}^{n+1} = \boldsymbol{f}(t^{n+1}) - (\boldsymbol{u}\cdot\nabla\boldsymbol{u})^{\star,n+1}$. Then solve

$$\Delta\phi^{n+1} = \nabla\cdot\tilde{\boldsymbol{u}}^{n+1}, \quad \partial_n\phi^{n+1}_{|\partial\Omega} = 0. \tag{54b}$$

And finally update the pressure as follows:

$$p^{n+1} = \tfrac{\beta_q}{\Delta t}\phi^{n+1} + p^{\star,n+1} - \nu\nabla\cdot\tilde{\boldsymbol{u}}^{n+1}. \tag{54c}$$

The algorithm (54a)–(54b)–(54c) is known in the literature as the rotational form of the pressure-correction method. Upon denoting $\mathsf{u}_{\Delta t} = (\boldsymbol{u}(t^0), \dots, \boldsymbol{u}(t^N))$ and $\mathsf{p}_{\Delta t} = (p(t^0), \dots, p(t^N))$, the above algorithm has been proved to yield the following error estimates

$$\|\mathsf{u}_{\Delta t} - \tilde{\boldsymbol{u}}_{\Delta t}\|_{\ell^2(L^2)} \le c\Delta t^2,$$
$$\|\nabla(\mathsf{u}_{\Delta t} - \tilde{\boldsymbol{u}}_{\Delta t})\|_{\ell^2(L^2)} + \|\mathsf{p}_{\Delta t} - p_{\Delta t}\|_{\ell^2(L^2)} \le c\Delta t^{\frac{3}{2}}.$$

where $\|\phi_{\Delta t}\|^2_{\ell^2(L^2)} = \Delta t \sum_{n=0}^N \int_\Omega |\phi^n|^2 \,\mathrm{d}\boldsymbol{x}$.

A simple strategy to initialize the algorithm consists of using $D^{(1)}\boldsymbol{u}^1$ at the first step in (54a), then using $D^{(2)}\boldsymbol{u}^2$ at the second step, and proceeding likewise until $\tilde{\boldsymbol{u}}^1, \dots, \tilde{u}^{q-1}$ have all been computed.

At the present time, projection methods count among the few methods that are capable of solving the time-dependent incompressible Navier–Stokes equations in three dimensions on fine meshes within reasonable computation times. The reason for this

success is that the unsplit strategy, which consists of solving

$$\text{(55a)} \qquad \tfrac{D^{(q)}}{\Delta t}\boldsymbol{u}^{n+1} - \nu\Delta\boldsymbol{u}^{n+1} + \nabla p^{n+1} = \boldsymbol{S}^{n+1},$$

$$\text{(55b)} \qquad \nabla{\cdot}\boldsymbol{u}^{n+1} = 0; \quad \boldsymbol{u}^{n+1}_{|\partial\Omega} = \boldsymbol{0},$$

yields a linear system similar to (37), which usually takes far more time to solve than sequentially solving (54a) and (54b). It is commonly reported in the literature that the ratio of the CPU time for solving (55a)–(55b) to that for solving (54a)–(54b)–(54c) ranges between 10 to 30.

See Also

Fluid Dynamics. Incompressible Euler equations. Newtonian fluids and thermohydraulics. Navier-Stokes turbulence. Partial differential equations in fluid mechanics. Variational methods in turbulence.

Further Reading

Doering, C.R.; Gibbon, J.D. (1995) *Applied analysis of the Navier-Stokes equations*. Cambridge Texts in Applied Mathematics. Cambridge: Cambridge University Press.

Ern A. and Guermond J.-L. (2004) *Theory and Practice of Finite Elements*. Springer Series in Applied Mathematical Sciences, Vol. **159**. New-York: Springer-Verlag.

Eymard R., Gallouët T., and Herbin, R. (2000) Finite volume methods. In: Ciarlet PG and Lions JL (eds.) *Handbook of numerical analysis*, Vol. **VII** 713–1020. Amsterdam: North-Holland.

Karniadakis, G.E.; Sherwin, S.J. (1999) *Spectral/hp element methods for CFD*. Numerical Mathematics and Scientific Computation. New York: Oxford University Press.

Rappaz M., Bellet M. and Deville M. (2003) *Numerical Modeling in Material Science and Engineering*. Springer Series in Computational Mathematics, Vol. **32**. Berlin: Springer-Verlag.

Temam, R. (1984) *Navier-Stokes equations. Theory and numerical analysis*. Studies in Mathematics and its Applications, Vol. **2**. Amsterdam: North-Holland.

Toro, E.F. (1997) *Riemann solvers and numerical methods for fluid dynamics. A practical introduction*. Berlin: Springer.

Wesseling, P. (2001) *Principles of computational fluid dynamics*. Springer Series in Computational Mathematics, Vol. **29**. Berlin: Springer.